



## Scholars Research Library

Der Pharma Chemica, 2012, 4 (1): 352-364  
(<http://derpharmachemica.com/archive.html>)



ISSN 0975-413X  
CODEN (USA): PCHHAX

# The Role of 3-Amino-2-Phenylimidazo[1,2-a]Pyridine as Corrosion Inhibitor for C38 Steel in 1M HCl

A. Ghazoui<sup>1</sup>, R. Saddik<sup>1</sup>, N. Benchat<sup>1</sup>, B. Hammouti<sup>1</sup>, M. Guenbour<sup>2</sup>, A. Zarrouk<sup>1</sup>, M. Ramdani<sup>1</sup>

<sup>1</sup>LCAE-URAC18, Faculté des Sciences, Université Mohammed Premier B.P. 717, 60000 Oujda, Morocco

<sup>2</sup>Laboratoire d'Electrochimie, Corrosion et Environnement, Faculté des Sciences, Rabat – Morocco

## ABSTRACT

3-amino-2-phenylimidazo[1,2-a]pyridine (P3) newly synthesised was tested as corrosion inhibitor of C38 steel in 1M HCl using weight loss method, potentiodynamic polarisation and electrochemical impedance spectroscopy (EIS) measurements. Gravimetric essays indicate that P3 inhibits the corrosion of steel. The effect is more pronounced with increasing of P3 concentration. The inhibition efficiency attains 92.8 % at the  $10^{-3}$ M. P3 affects both cathodic and anodic current and then limits  $H^+$  reduction and iron dissolution. P3 may be classified as a mixed inhibitor. EIS diagrams show that adsorption of P3 increases the transfer resistance and decrease the capacitance of interface metal/solution. Langmuir isotherm is the best fitted adsorption one to describe P3 action on steel surface. The negative values of  $\Delta G_{ads}^{\circ}$  indicate the spontaneous adsorption of the inhibitor on steel surface. Both kinetic parameters (activation energy, pre-exponential factor, enthalpy of activation and entropy of activation) were calculated and discussed.

**Keywords:** Corrosion; Imidazopyridine; HCl; C38 steel; Potentiodynamic polarisation; EIS.

## INTRODUCTION

Hydrochloric acid solutions are widely used in chemical and several industrial processes such as acid pickling, acid cleaning, acid descaling and oil well acidizing, which require the use of corrosion inhibitors [1-5].

N-heterocyclic compounds are well qualified to play more protection for steel corrosion [6-8]. Many N-heterocyclic compounds such as derivatives of pyrazole [9-11], bipyrazole [12-14], triazole [15-17], tetrazole [18-20], imidazole [21-24], pyridine [25-28], pyrimidine [29], pyridazine [30-32] and imidazopyridine [33] have been reported as effective corrosion inhibitors for steel in acidic media. The heterocyclic compound containing nitrogen atoms can easily be protonated in acidic medium to exhibit good inhibitory action on the corrosion of metals in acid solutions.

The present study aimed to test a new compound named 3-amino-2-phenylimidazo[1,2-a]pyridine (P3) on the corrosion of mild steel in 1.0 M hydrochloric acid solution. The study has

been evaluated using weight loss, potentiodynamic polarization and EIS techniques at various concentrations ( $1 \times 10^{-6}$ – $1 \times 10^{-3}$  M) of P3. The adsorption of P3 was also studied to show that inhibitor adsorb on the steel surface according to the Langmuir isotherm.

## MATERIALS AND METHODS

3-amino-2-phenylimidazo[1,2-a]pyridine (P3) was synthesised according to the following procedure (Fig. 1): To a suspension of tin (1g) in ice-cold concentrated HBr (30ml) was added during 0.5h 3-nitroso-2-phenyl imidazo[1,2-a]pyridine with stirring. After being stirred for 3h the precipitate was filtered taken up in H<sub>2</sub>O (30ml) and the suspension made alkaline with NH<sub>4</sub>OH. The solid was extracted overnight with in CH<sub>2</sub>Cl<sub>2</sub> in a soxhlet apparatus. The CH<sub>2</sub>Cl<sub>2</sub> was dried (Na<sub>2</sub>SO<sub>4</sub>) and filtered and the solvent evaporated, producing compounds which were recrystallized from CHCl<sub>3</sub> to give yellow crystals.

Melting point: 212-213 °C.

MS (EI, *m/z*): 209 (M+).

IR (KBr, cm<sup>-1</sup>): 3400 (NH<sub>2</sub>), 1630, 750.

<sup>1</sup>H NMR (CDCl<sub>3</sub>, 300 MHz): 8.46 (m, 1H); 8.10 (m, 2H); 7.46 (m, 5H); 7.15 (t, 1H) 3.80(NH<sub>2</sub>)

Molar HCl solutions were prepared by dilution of analytical grade 37 % HCl with bidistilled water. Prior to all measurements, the steel samples were polished with different emery paper up to 1200 grade and washed thoroughly with bidistilled water and dried with acetone. The concentration range of this compounds was  $10^{-6}$  to  $10^{-3}$  M.

Gravimetric measurements were carried out in a double-walled glass cell equipped with a thermostat cooling condenser. The solution volume was 50 mL. The steel specimens used had a rectangular form (1cm × 1cm × 0.05cm). The immersion time for the weight loss was 6 h at 308 K. the inhibition efficiency ( $E_w$  %) determined by the following equation:

$$E_w \% = \left( 1 - \frac{W_{corr}}{W_{corr}^{\circ}} \right) \times 100 \quad (1)$$

Where  $W_{corr}$  and  $W_{corr}^{\circ}$  are the corrosion rates of steel in the presence and absence of P3, respectively.

Electrochemical experiments were recorded by using an Radiometer analytical (Voltalab-PGZ 301), coupled to a computer equipped with a software Voltmaster 4.

A three electrode electrochemical cell was used. The working electrode was Steel with the different surfaces area. Before each experiment, the electrode was polished using emery paper until 1200 grade. After this, the electrode was cleaned ultrasonically with distillate water.

All potentials were given with reference to the saturated calomel electrode (SCE). The counter electrode was platinum.

The working electrode was immersed in test solution during 30 minutes until a steady state open circuit potential ( $E_{ocp}$ ) was obtained. The polarization curve was recorded by polarization from - 800 mV to 500 mV under potentiodynamic conditions corresponding to 1 mV/s (sweep rate) and under air atmosphere.  $E\%$  was calculated using the equation 2:

$$E_I \% = \frac{I_{corr} - I_{corr(inh)}}{I_{corr}} \times 100 \quad (2)$$

where  $I_{corr}$  and  $I_{corr(inh)}$  are the corrosion current density values without and with inhibitor, respectively.

The electrochemical impedance spectroscopy measurements were carried out using a transfer function analyser (Analytical Radiometer PGZ 301), with a small amplitude ac. Signal (10 mV), over a frequency domain from 100 KHz to 100 mHz at 308 K and an air atmosphere. The polarization resistance  $R_p$ , is obtained from the diameter of the semicircle in Nyquist representation. In this case, the inhibition efficiency is calculated using charge transfer resistance from equation 3:

$$E_R \% = \frac{R_{ct} - R_{ct(inh)}}{R_{ct}} \times 100 \quad (3)$$

where  $R_{ct(inh)}$  and  $R_{ct}$  are the charge transfer resistance in the presence and absence of P3, respectively.

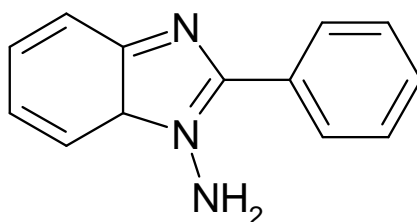


Figure 1. Molecular structure of the 3-amino-2-phenylimidazo[1,2-a]pyridine (P3)

## RESULTS AND DISCUSSION

### 3.1. Gravimetric measurements

#### 3.1.1. Effect of concentration

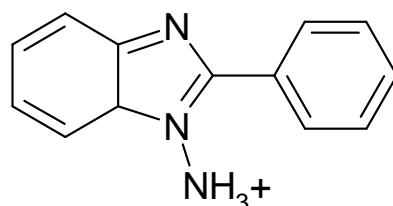
The evolution of corrosion rate of steel in 1M HCl solutions was determined by weight loss measurement at 6 h of immersion at different P3 concentrations. Table 1 collects the values of corrosion rate and the corresponding efficiency.

Table 1. Gravimetric results of C38 steel in 1M HCl at different concentration of each inhibitor at 6h and 308 K.

Inhibitors	Conc (M)	$W_{corr}$ (mg/cm <sup>2</sup> .h)	$E_w$ (%)	$\theta$
Blank	1	1.14	----	----
P3	$1 \times 10^{-6}$	0.6166	45.9	0.459
	$1 \times 10^{-5}$	0.4134	63.7	0.637
	$5 \times 10^{-5}$	0.2994	73.7	0.737
	$1 \times 10^{-4}$	0.2720	76.1	0.761
	$5 \times 10^{-4}$	0.1293	88.7	0.887
	$1 \times 10^{-3}$	0.0823	<b>92.8</b>	<b>0.928</b>

Examination of vales indicates clearly a net decrease in the corrosion rate of steel in the presence of P3. In other words, its inhibition efficiency increased to reach the higher value of 92.8% at  $10^{-3}$ M. This may be interpreted by the presence of seven double bonds near three nitrogen atoms.

The amine group is easily protonated in acidic medium to give ammonium cation well known in literature to promote inhibition of steel [34-36]:



The presence of this kind of cyclic rings and nitrogen atoms facilitates the adsorption process.

The variations in the degree of surface coverage and corrosion rate with P3 concentration shown in Fig 2 suggest that P3 inhibits steel at all the concentration range used in the study. Maximum degree of surface coverage was reported at 10<sup>-3</sup>M concentration of this compound.

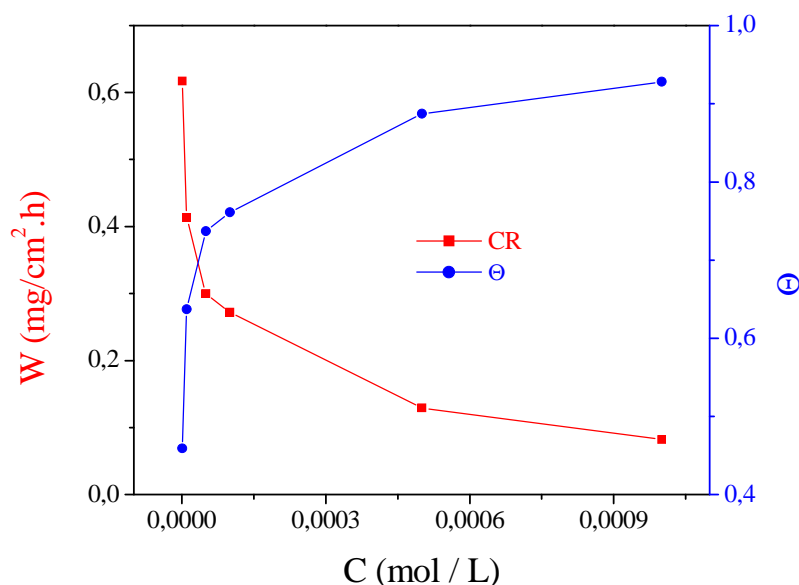


Figure 2. Variation of inhibition efficiency and corrosion rate in 1M HCl on C38 steel surface without and with different concentrations of P3.

### 3.1.2. Adsorption isotherm and thermodynamic parameters

The adsorption on the corroding surfaces never reaches the real equilibrium and tends to reach an adsorption steady state. However, when the corrosion rate is sufficiently small, the adsorption steady state has a tendency to become a quasi-equilibrium state. In this case, it is reasonable to consider the quasi-equilibrium adsorption in thermodynamic way using the appropriate equilibrium isotherms [37]. The efficiency of this compound as a successful corrosion inhibitor mainly depends on its adsorption ability on the metal surface. So, it is essential to know the mode of adsorption and the adsorption isotherm that can give valuable information on the interaction of inhibitor and metal surface. The surface coverage values,  $\Theta$  ( $\Theta = IE/100$ ) for different concentrations of P3 was used to explain the best adsorption isotherm. A plot of  $C/\Theta$  versus  $C$  (Fig. 3) gives a straight line with an average correlation coefficient of 0.99967 and a slope of nearly unity (1.07) suggests that the adsorption of P3 molecules obeys Langmuir adsorption isotherm, which can be expressed by the following equation 4:

$$\frac{C}{\Theta} = \frac{1}{K} + C \quad \text{with} \quad (4)$$

Where K is the adsorptive equilibrium constant, C is the inhibitor concentration.

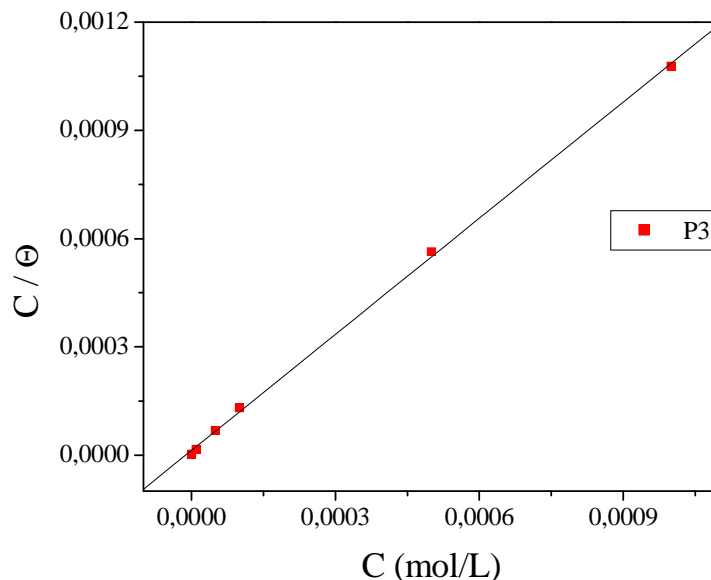


Figure 3. Langmuir adsorption of P3 on the steel surface in HCl solution

The thermodynamic parameters from the Langmuir adsorption isotherm are listed in Table 2, together with the value of the Gibbs free energy of adsorption  $\Delta G_{ads}^{\circ}$  calculated from the equation:

$$\Delta G_{ads}^{\circ} = -RT \ln(55.5 K_{ads}) \quad (5)$$

Where R is the universal gas constant, T the thermodynamic temperature and the value of 55.5 is the concentration of water in the solution [38].

The value  $K_{ads}$  calculated from the reciprocal of intercept of isotherm line as  $7.938524 \times 10^4 \text{ M}^{-1}$ . The high value of the adsorption equilibrium constant reflects the high adsorption ability of this inhibitor on C38 steel surface.

Table 2. Thermodynamic parameters for the adsorption of P3 in 1M HCl on the C38 steel at 308K

Inhibitor	Slope	$K_{ads} (\text{M}^{-1})$	$R^2$	$\Delta G_{ads}^{\circ} (\text{kJ/mol})$
P3	1.07	79385.24	0,99967	-39.17

From Eq. (5),  $\Delta G_{ads}^{\circ}$  was calculated as  $-39.17 \text{ kJ mol}^{-1}$ . The negative value of standard free energy of adsorption indicates spontaneous adsorption of P3 molecules on C38 steel surface and also the strong interaction between inhibitor molecules and the metal surface [39, 40]. Generally, the standard free energy values of  $-20 \text{ kJ mol}^{-1}$  or less negative are associated with an electrostatic interaction between charged molecules and charged metal surface (physical adsorption); those of  $-40 \text{ kJ mol}^{-1}$  or more negative involves charge sharing or transfer from the

inhibitor molecules to the metal surface to form a co-ordinate covalent bond (chemical adsorption) [41, 42]. The value of  $\Delta G_{ads}^{\circ}$  in our measurement is  $-39.17 \text{ kJ mol}^{-1}$  (in Table 2), it is suggested that the adsorption of this P3 derivative involves two types of interactions: chemisorption and physisorption [43].

### 3.1.3. Effect of temperature and thermodynamic activation parameters

In order to study the effect of temperature on the inhibition efficiencies of P3, weight loss measurements were carried out in the temperature range 308–343K in absence and presence of inhibitor at optimum concentration. The corresponding data are shown in Table 3.

The degree of surface coverage ( $\Theta$ ) was calculated using equation 6:

$$\Theta = 1 - \frac{W_{corr}}{W_{corr}^{\circ}} \quad (6)$$

**Table 3. Various corrosion parameters for steel in 1M HCl in absence and presence of optimum concentration of P3 at different temperatures at 1h**

Temperature (K)	Inhibitor	W(mg/cm <sup>2</sup> .h)	E <sub>w</sub> (%)	$\Theta$
308	Blank	1.142	-	-
	P3	0.082	92.80	0.928
313	Blank	1.580	-	-
	P3	0.150	90.50	0.905
323	Blank	3.030	-	-
	P3	0.479	84.20	0.842
333	Blank	5.150	-	-
	P3	1.365	73.50	0.735
343	Blank	9.000	-	-
	P3	3.645	59.50	0.595

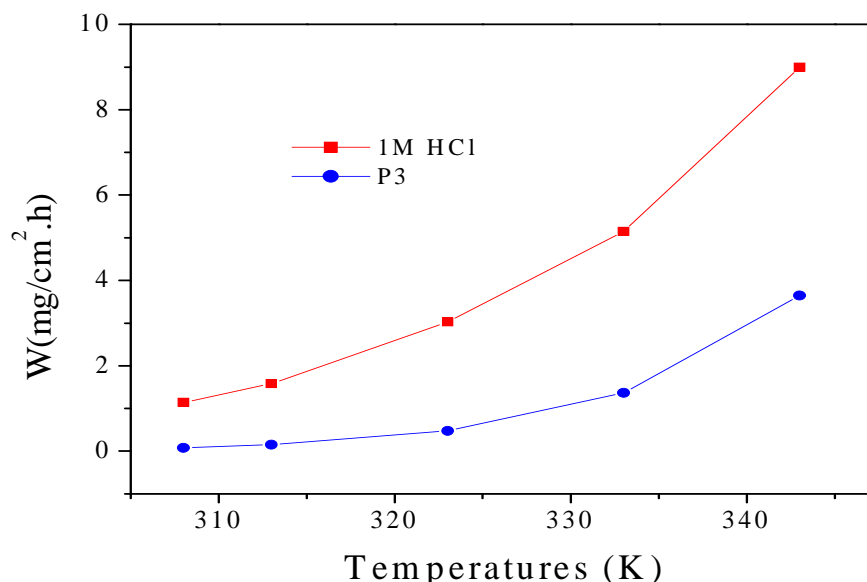


**Fig 4. Variation of corrosion rate in 1M HCl on steel surface without and with of optimum concentration of pyridazine at different temperatures**

Inspection of Table 3 showed that corrosion rate increased with increasing temperature both in uninhibited and inhibited solutions while the inhibition efficiency of P3 decreased with

temperature. A decrease in inhibition efficiencies with the increase temperature in presence of P3 might be due to weakening of physical adsorption.

In order to calculate activation parameters for the corrosion process, Arrhenius Eq. (7) and transition state Eq. (8) were used [44]:

$$C_R = A \exp\left(\frac{-E_a}{RT}\right) \quad (7)$$

$$C_R = \frac{RT}{Nh} \exp\left(\frac{\Delta S_a^\circ}{R}\right) \exp\left(-\frac{\Delta H_a^\circ}{RT}\right) \quad (8)$$

Where  $C_R$  is the corrosion rate,  $R$  the gas constant,  $T$  the absolute temperature,  $A$  the pre-exponential factor,  $h$  the Plank's constant and  $N$  is Avogrado's number,  $E_a$  the activation energy for corrosion process,  $\Delta H_a^\circ$  the enthalpy of activation and  $\Delta S_a^\circ$  the entropy of activation.

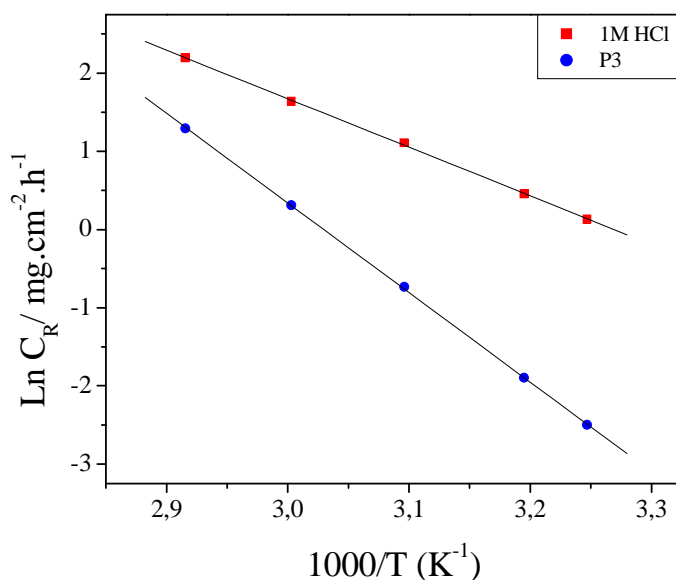


Fig. 5. Arrhenius plots of  $\text{Ln } C_R$  vs.  $1/T$  for steel in 1M HCl in the absence and the presence of P3 at optimum concentration.

The apparent activation energy ( $E_a$ ) at optimum concentration of P3 was determined by linear regression between  $\text{Ln } C_R$  and  $1/T$  (Fig. 5) and the result is shown in Table 4. The linear regression coefficient was close to 1, indicating that the steel corrosion in hydrochloric acid can be elucidated using the kinetic model. Inspection of Table 4 showed that the value of  $E_a$  determined in 1M HCl containing P3 is higher (95.29 kJ mol<sup>-1</sup>) than that for uninhibited solution (51.64 kJ mol<sup>-1</sup>). The increase in the apparent activation energy may be interpreted as physical adsorption that occurs in the first stage [45]. Szauer and Brand explained that the increase in activation energy can be attributed to an appreciable decrease in the adsorption of the inhibitor on the steel surface with increase in temperature. As adsorption decreases more desorption of inhibitor molecules occurs because these two opposite processes are in equilibrium. Due to more desorption of inhibitor molecules at higher temperatures the greater surface area of steel comes

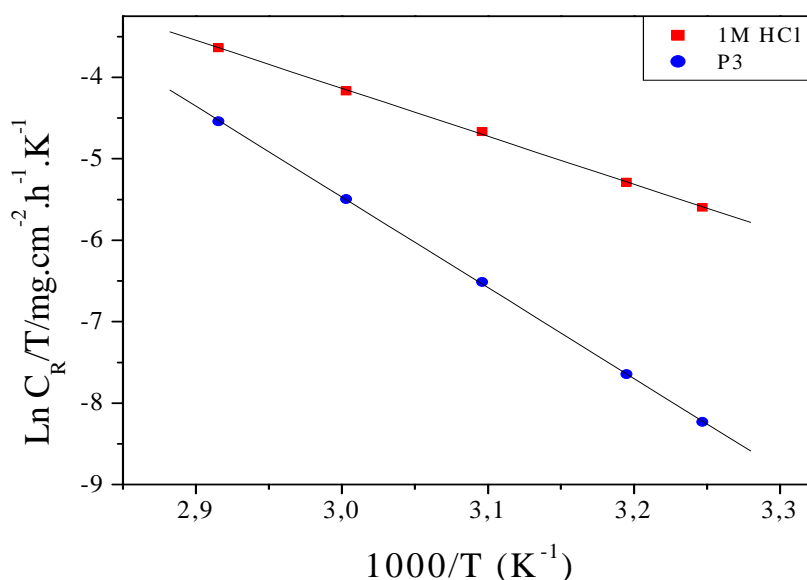
in contact with aggressive environment, resulting increased corrosion rates with increase in temperature [46].

Fig. 6 showed a plot of  $\ln(C_R/T)$  versus  $1/T$ . The straight lines are obtained with a slope ( $\Delta H_a^\circ/R$ ) and an intercept of  $(\ln R/Nh + \Delta S_a^\circ/R)$  from which the values of the values of  $\Delta H_a^\circ$  and  $\Delta S_a^\circ$  are calculated and are given in Table 4. Inspection of these data revealed that the thermodynamic parameters ( $\Delta H_a^\circ$  and  $\Delta S_a^\circ$ ) for dissolution reaction of steel in 1M HCl in the presence of P3 is higher ( $92.59 \text{ kJ mol}^{-1}$ ) than that of in the absence of inhibitor ( $48.95 \text{ kJ mol}^{-1}$ ). The positive sign of  $\Delta H_a^\circ$  reflect the endothermic nature of the steel dissolution process suggesting that the dissolution of steel is slow [47] in the presence of inhibitor.

**Table 4. Activation parameters for the steel dissolution in 1M HCl in the absence and the presence of P3 at optimum concentration**

Inhibitor	A ( $\text{mg/cm}^2 \cdot \text{h}$ )	Linear regression coefficient (r)	$E_a$ (kJ/mol)	$\Delta H_a^\circ$ (kJ/mol)	$\Delta S_a^\circ$ (J/mol.K)
Blank	$6,6071 \times 10^8$	0,99977	51.64	48.95	-85.09
P3	$1.2023 \times 10^{15}$	0,99995	95.29	92.59	34.75

The large negative value of  $\Delta S_a^\circ$  for C38 steel in 1M HCl implies that the activated complex is the rate-determining step, rather than the dissociation step. In the presence of the inhibitor, the value of  $\Delta S_a^\circ$  increases and is generally interpreted as an increase in disorder as the reactants are converted to the activated complexes [18]. The positive values of  $\Delta S_a^\circ$  reflect the fact that the adsorption process is accompanied by an increase in entropy, which is the driving force for the adsorption of the inhibitor onto the steel surface.



**Fig. 6. Arrhenius plots of  $\ln C_R/T$  vs.  $1/T$  for steel in 1M HCl in the absence and the presence of P3 at optimum concentration.**

### 3.2. Polarization curves

The polarization curves of C38 steel in 1M HCl obtained with and without various concentrations of used inhibitor are shown in Fig.7. Electrochemical parameters such as corrosion current density ( $I_{\text{corr}}$ ), corrosion potential ( $E_{\text{corr}}$ ), Tafel slope constants calculated from Tafel plots ( $-\beta_c$ ) and the inhibition efficiency ( $E_I$  %) were determined by Tafel extrapolation method and are given in Table 5.

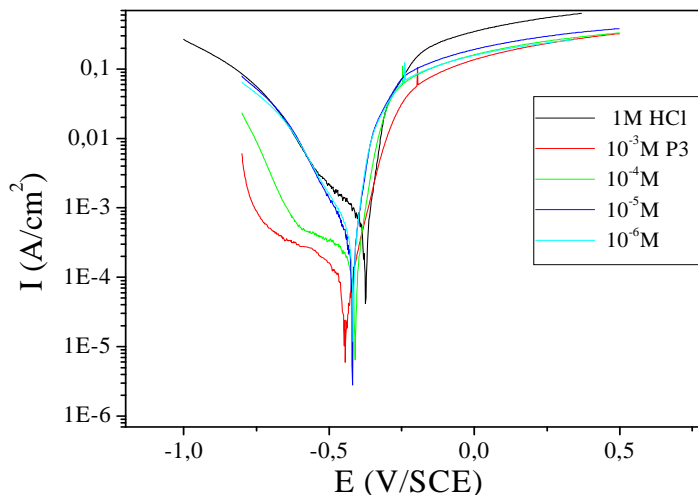


Figure 7. Polarization curves of C38 steel in 1M HCl containing different concentrations of P3.

It is seen that the addition of various inhibitor affects the polarization curves and consequently decreases  $I_{\text{corr}}$  significantly, due to increase in the blocked fraction of electrode surface by adsorption. Cathodic curves gave rise to parallel Tafel lines indicating that the hydrogen evolution is activation controlled and the reduction mechanism is not affected by the presence of inhibitor. In another hand, we note that the addition of products did not change the corrosion potential values ( $E_{\text{corr}}$ ) for all concentration. These results demonstrated that the hydrogen evolution reaction was inhibited and that the inhibition efficiency increased with inhibitor concentration.

In the anodic domain, the presence of P3 decreases anodic current density, the highest effect is observed with P3 increase of the over voltage near the corrosion potential. For an over voltage higher than -200 mV/SCE, the presence of this inhibitor does not change the current density-potential characteristics. This fact means that the inhibition mode of the pyridazine depends upon electrode potential.

Table 5. Polarization data of C38 steel in 1M HCl without and with addition of inhibitor at 308 K

Inhibitor	Conc (M)	$-E_{\text{corr}}$ (mV/SCE)	$-\beta_c$ (mV/dec)	$I_{\text{corr}}$ ( $\mu\text{A}/\text{cm}^2$ )	$E_I$ (%)
Blank	1	375.7	217.2	814.2	-- ----
P <sub>3</sub>	$10^{-6}$	418.1	151.6	448.3	44.9
	$10^{-5}$	418.1	131.5	314.1	61.4
	$10^{-4}$	410.8	437.5	192.0	76.4
	$10^{-3}$	446.4	258.5	091.4	<b>88.8</b>

### 3.3. Electrochemical impedance spectroscopic studies

The corrosion behaviour of C38 steel, in acidic solution containing different concentration of pyridazine compound, was investigated by the electrochemical impedance spectroscopy (EIS) at 308 K after 30 min of immersion. The obtained results are presented in Fig.8. The impedance parameters calculated are given in Table 6. The diagrams are composed of one capacitive loop.

The charge-transfer resistance values ( $R_{ct}$ ) were calculated from the difference in real impedance at lower and higher frequencies as suggested by Tsuru et al. [48]. To obtain the double-layer capacitance ( $C_{dl}$ ), the frequency at which the imaginary component of the impedance is maximum ( $-Z_{i_{max}}$ ) is found and  $C_{dl}$  values were obtained from the equation 6:

$$f(-Z_{i_{max}}) = \frac{1}{2\pi C_{dl} R_{ct}} \quad (8)$$

Results obtained show that  $R_{ct}$  increases and  $C_{dl}$  tends to decrease with increasing of inhibitor concentration.

A decrease in the  $C_{dl}$  values with increase of the concentration of inhibitor (Fig. 9). This phenomenon is generally related to the adsorption of organic molecules on the metal surface and then leads to a decrease in the local dielectric constant and/or an increase in the thickness of the electrical double layer [49].

$$C_{dl} = \frac{\epsilon_o \epsilon}{\delta} S \quad (9)$$

Where  $\delta$  is the thickness of the protective layer,  $S$  is the electrode area,  $\epsilon_o$  the vacuum permittivity of vide and  $\epsilon$  is dielectric constant of the medium.

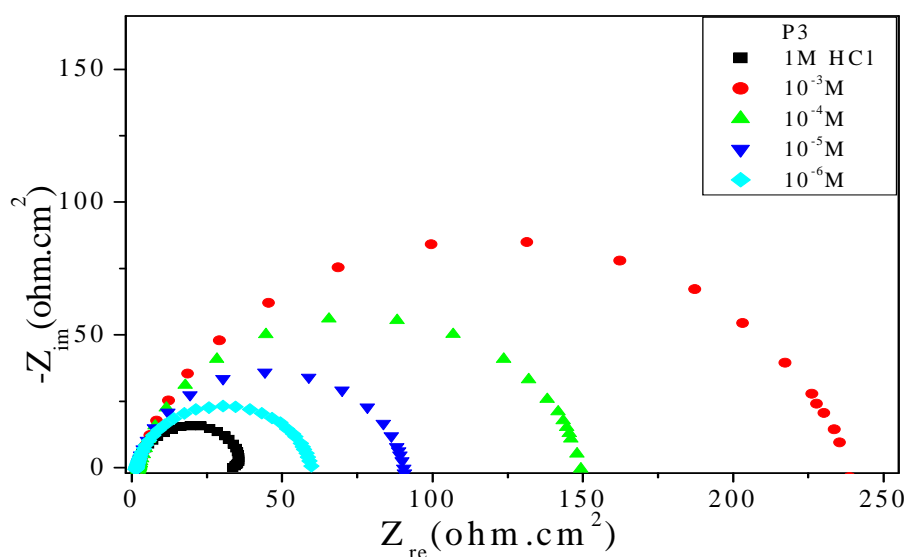


Figure 8. Nyquist diagrams C38 steel in 1M HCl without and with different concentrations of inhibitor.

Table 6. Impedance parameters of C38 steel in 1M HCl containing different concentrations of P3 compound

Inhibitor	Conc (M)	$R_{ct}$ ( $\Omega.cm^2$ )	$F_{max}$ (Hz)	$C_{dl}$ ( $\mu F.cm^{-2}$ )	$E_{Rct}$ (%)
Blank	1	033.2	50.00	095.8	-----
P3	$10^{-6}$	059.7	25.00	106.5	44.4
	$10^{-5}$	091.0	31.6	055.3	63.5
	$10^{-4}$	149.3	25.0	042.7	77.75
	$10^{-3}$	238.8	20.0	033.3	86.1

A low capacitance may result if water molecules at the electrode interface are largely replaced by organic inhibitor molecules through adsorption [50]. The larger inhibitor molecules also reduce the capacitance through the increase in the double layer thickness [51]. The inhibiting effectiveness increases with the concentration of the inhibitor to reach a maximum value from 86.1 % to  $10^{-3}$  M.

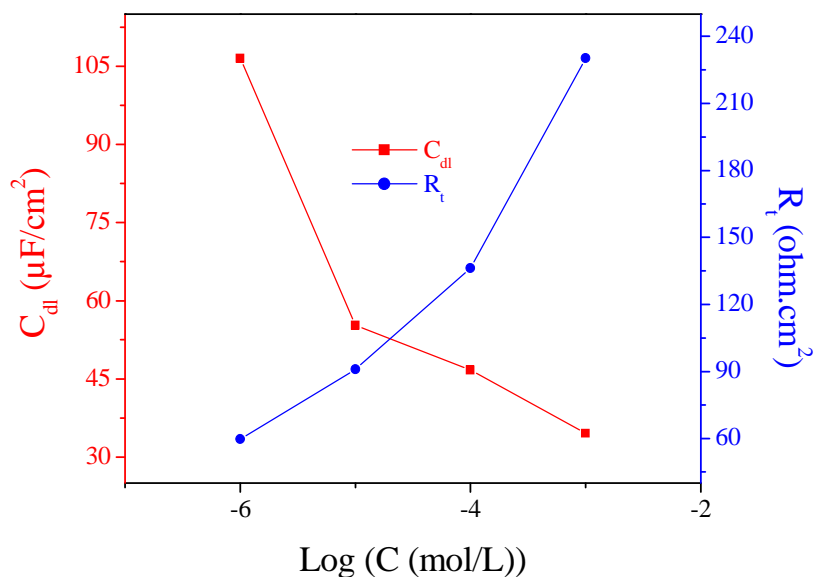


Figure .9. Evolution of transfer resistance and capacitance as function of logarithm of P3 concentration

A comparison may be made between inhibition efficiency  $E$  (%) values obtained by different methods (weight loss, polarisation curves and EIS methods). Fig 10 shows a curve that compares the

$E$  (%) values obtained. One can see that whatever the method used, no significant changes are observed in  $E$  (%) values. We can then conclude that there is a good correlation with the three methods used in this investigation at all tested concentrations and that P3 is an efficient corrosion inhibitor.

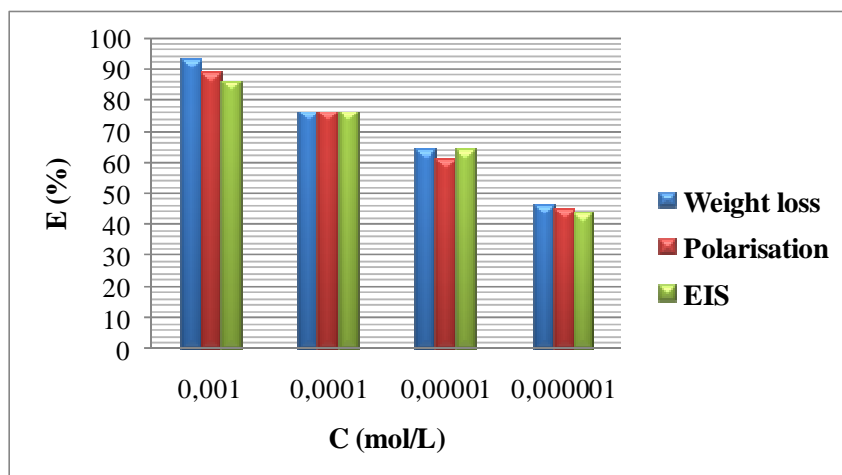


Figure 10. Comparison of inhibition efficiency ( $E$  %) values obtained by weight loss, polarisation and EIS methods

## CONCLUSION

On the basis of these results, the following conclusions may be drawn:

- P3 inhibit the corrosion of C38 steel in 1M HCl. The inhibition efficiency depends on the molecular structure.
- The inhibition efficiency increases with increasing inhibitor concentrations to attain a maximum value of 92.78 % for inhibitor P3 at  $10^{-3}$  M.
- The negative values of  $\Delta G_{ads}^{\circ}$  indicate that the adsorption of the inhibitor molecule is a spontaneous process and an adsorption mechanism is typical of chemisorption and physisorption.
- The inhibition efficiency decreased with increasing temperature as a result of the higher dissolution of steel at higher temperature.
- Kinetic and adsorption parameters were evaluated and discussed.
- Polarization study shows that Imidazopyridine act as mixed-type inhibitors for an over voltage inferior than  $-440$  mV/SCE.
- Impedance method indicates that Imidazopyridine compounds adsorbs on C38 steel surface with increasing charge transfer resistance and decreasing the double-layer capacitance.

## REFERENCES

- [1] M. Batros and N. Hakerman, *J. Electrochem. Soc.*, **1992**, 139, 3429
- [2] F. Bentiss, M. Lagrenee, M. Traisnel, B. Mernari, and H. El Attari, *J. Appl. Electrochem.* **1999**, 29, 1073
- [3] P. Kutej, J. Vosta, J. Pancir, J. Macak, and N. Hackerman, *J. Electrochem. Soc.*, **1995**, 142, 829
- [4] M. Dahmani, A. Et-Touhami, S.S. Al-Deyab, B. Hammouti and A. Bouyanzer, *Int. J. Electrochem. Sci.*, **2010**, 5, 1060.
- [5] J.M. Bastidas, J.L. Polo and E. Cano, *J. Electrochem. Soc.*, **2000**, 30, 1173
- [6] B. Hammouti, A. Zarrouk, S.S. Al-Deyab and I. Warad, *Oriental J. Chem.* **2011**, 27, 23.
- [7] E.E. Foad El Sherbini, *Mater. Chem. Phys.*, **1999**, 60, 286
- [8] W.W. Frenier, F.B. Growcock and V.R. Lopp, *Corrosion*, **1988**, 44, 590
- [9] M.A. Quraishi and D. Jamal, *Corrosion*, **2000**, 56, 156
- [10] M. Benabdellah, A. Yahyi, A. Dafali, A. Aouniti, B. Hammouti and A. Ettouhami, *Arab. J. Chem.* **2011**, 4, 343.
- [11] M. Elayyachy, B. Hammouti, A. El Idrissi and A. Aouniti, *Portugaliae Electrochimica Acta*, **2011**, 29, 57.
- [12] J.M. Sykes, *Br. Corros. J.*, **1990**, 25, 175
- [13] P. Chatterjee, M.K. Banerjee and K.P. Mukherjee, *Indian J. Technol.* **1991**, 29, 191
- [14] JO'M. Bockris, and B. Yang, *J. Electrochem. Soc.*, **1991**, 138, 2237
- [15] A.Zarrouk, I. Warad, B. Hammouti, A. Dafali, S.S. Al-Deyab and N. Benchat, *Int. J. Electrochem. Sci.*, **2010**, 5, 1516.
- [16] DA. Vermilyea, in, First International Congress; Metal Corrosion; Butterworths; London; **1962**, p 62
- [17] F. Bentiss, M. Traisnel, N. Chaibi, B. Mernari, H. Vezin and M. Lagrenee, *Corros. Sci.*, **2002**, 44, 2271
- [18] I.El Ouali, B. Hammouti, A. Aouniti, Y. Ramli, M. Azougagh, E.M., Essassi and M. Bouachrine, *J. Mater. Environ. Sci.* **2010**, 1, 1.
- [19] K.F. Khaled, N.S. Abdelshafi, A. El-Maghraby and N. Al-Mobarak, *J. Mater. Environ. Sci.* **2011**, 2, 166.
- [20] J. Uhrea and K. Aramaki, *J. Electrochem. Soc.*, **1991**, 138, 3245
- [21] S. Kertit and B. Hammouti, *Appl. Surf. Sci.*, **1996**, 93, 59

- [22] A.Chetouani, B. Hammouti, A. Aouniti, N. Benchat and T. Benhadda, *Prog. Org. Coat.*, **2002**, 45, 373
- [23] K. Bekkouch, A. Aouniti, B. Hammouti, S. Kertit, *J. Chim. Phys.*, **1999**, 96, 838
- [24] S. Kertit, B. Hammouti, M. Taleb and M.; Brighli, *Bull. Electrochem.* **1997**, 13, 241
- [25] M. Bouklah, N. Benchat, A. Aouniti, B. Hammouti, M. Benkaddour, M. Lagrenee, H. Vezin and F. Bentiss, *Prog. Org. Coat.*, **2004**, 51,118
- [26] L. Wang, *Corros. Sci.*, **2006**, 48, 608
- [27] M. Lagrenee, B. Mernari, N. Chaibi, M. Traisnel, H. Vezin and F. Bentiss, *Corros. Sci.*, **2001**, 43, 951
- [28] S. Rengamani, S. Muralidharan, M. Anbu Kulandainathan and S. Venkatakrishna Iyer, *J. Electrochem. Soc.*, **1994**, 24, 355
- [29] F. Bentiss, F. Gassama, D. Barbry, L. Gengembre, H. Vezin, M. Lagrenée, M. Traisnel, *Appl. Surf.Sci.* **2006**, 252, 2684.
- [30] A.Chetouani, B. Hammouti, A. Aouniti, N. Benchat, T. Benhadda, *Prog. Org. Coat.* **2003**, 45, 73.
- [31] A.Chetouani, A. Aouniti, B. Hammouti, N. Benchat, T. Benhadda, S. Kertit, *Corros. Sci.* **2003**, 45, 1675.
- [32] N.A. Negm, A.M. Al Sabagh, M.A. Migahed, H.M. Abdel Bary, H.M. El Din, *Corros. Sci.*, **2010**, 52, 2122.
- [33] Qi Zhang, Zhinong Gao, Feng Xu, Xia Zou, *Colloids and Surfaces A: Physicochemical and Engineering Aspects* **2011**, 380, 191.
- [34] A. Popova, M. Christov, A. Vasilev, *Corros. Sci.* **2011**, 53, 1770.
- [35] L.J. Vracar, D.M. Drazic, *Corros. Sci.* **2002**, 44, 1669–1680.
- [36] O. Olivares, N. V. Likhanova, B. Gomez, J. Navarrete, M.E. Llanos-Serrano, E. Arce, J.M. Hallen, *Appl. Surf. Sci.* **2006**, 252, 2894.
- [37] G. Avci, *Mater. Chem. Phys.* **2008**, 112, 234.
- [38] E. Bayol, A.A. Gurten, M. Dursun, K. Kayakırılmaz, *Acta Phys. Chim. Sin.* 24 (**2008**) 2236.
- [39] O.K. Abiola, N.C. Oforka, , *Mater. Chem. Phys.* **2004**, 83, 315–322.
- [40] M. Ozcan, R. Solmaz, G. Kardas, I. Dehri, *Colloid Surf. A* **2008**, 325, 57.
- [41] S. Zhang, Z. Tao , W. Li, B. Hou, *Appl. Surf. Sci.* **2009**, 255, 6757.
- [42] J.O'M. Bockris, A.K.N. Reddy, *Modern Electrochemistry, Plenum Press, New York*, **1977**, 2, 1267.
- [43] S. Martinez, I. Stern, *Appl. Surf. Sci.* **2002**, 199, 83.
- [44] T. Szauer, A. Brand, *Electrochim. Acta* **1981**, 26, 1219.
- [45] N.M. Guan, L. Xueming, L. Fei, *Mater. Chem. Phys.* **2004**, 86, 59.
- [46] T. Tsuru, S. Haruyama, B. Gijutsu, *J. Jpn. Soc. Corros. Eng.* **1978**, 27, 573.
- [47] E. McCafferty, N. Hackerman, *J. Electrochem. Soc.* **1972**, 119, 146.
- [48] P. Li, J. Y. Lin, K. L. Tan, J. Y. Lee, *Electrochim. Acta* **1997**, 42, 605.
- [49] S. S. Abdel Rehim, O. A. Hazzazi, M. A. Amin, K. F. Khaled, *Crros. Sci.*, **2008**, 50, 2258.